The Bioscan AN INTERNATIONAL QUARTERLY JOURNAL OF LIFE SCIENCES 21(2): 22619-22630, 2026 www.thebioscan.com

Electrochemical and Surface-Analytical Investigation of Sodium Gluconate–Mn^{2+} Synergism for Carbon-Steel Corrosion Control

Angel J.B. Ponmalar† and S. Sudha Kumari*

†Research Scholar (Reg. Number: 21113152032011), Department of Chemistry, S.T. Hindu College, Nagercoil, Tamil Nadu – 629 002.

*Associate Professor, Department of Chemistry, S.T. Hindu College, Nagercoil, Tamil Nadu – 629 002.
†&* Affiliated to Manonmaniam Sundaranar University, Tirunelveli-12, Tamil Nadu, India.

DOI: https://doi.org/10.63001/tbs.2026.v21.i02.pp22619-22630

KEYWORDS

carbon steel, groundwater, sodium gluconate, Mn^{2+}, synergistic inhibition, electrochemical impedance spectroscopy, FTIR, protective film

Article Info

Received: 30.05.2026

Accepted: 18.06.2026

Published: 28.06.2026

Abstract

Groundwater serves as an important source of water for industrial applications; however, its dissolved oxygen and salts can accelerate the corrosion of carbon steel. This study investigates the synergistic corrosion inhibition effect of sodium gluconate (SG) combined with Mn^{2+} ions on carbon steel immersed in groundwater collected from Tirunelveli, Tamil Nadu, India. The inhibition efficiency and protective film characteristics were assessed using weight-loss measurements, potentiodynamic polarization, electrochemical impedance spectroscopy (EIS), Fourier-transform infrared spectroscopy (FTIR), and surface microscopy. The groundwater exhibited a pH of 8.0, a total dissolved solids concentration of 810 mg L^{-1}, and chloride and sulphate concentrations of 15 and 17 mg L^{-1}, respectively. According to the original experimental dataset, the SG–Mn^{2+} formulation demonstrated pronounced synergistic inhibition, achieving a maximum inhibition efficiency of 97.56% at concentrations of 200 ppm SG and 50 ppm Mn^{2+} after three days of immersion. Under these conditions, the charge-transfer resistance increased from 5.12 to 298.345 Ω cm^2, whereas the double-layer capacitance decreased from 1.7×10^{-2} to 1.3×10^{-5} F cm^{-2}, indicating the formation of a more resistive protective layer on the metal surface. FTIR analysis suggested the formation of an Fe^{2+}–gluconate surface complex in association with $Mn(OH)_2$. These findings are considered in the context of recent advances in sustainable corrosion protection and synergistic inhibitor formulations for carbon steel in aqueous environments. Overall, the SG–Mn^{2+} combination shows promise as a comparatively low-dose corrosion inhibitor and warrants further investigation for potential applications in groundwater systems and industrial cooling-water environments.

1. Introduction

Carbon steel is extensively used in pipelines, heat exchangers, storage equipment and other water-handling components because of its low cost, strength and ease of fabrication. Its exposure to aerated aqueous environments, however, makes it susceptible to electrochemical corrosion. In industrial water systems, dissolved oxygen, chloride, sulphate, alkalinity and other dissolved species can influence both the rate and morphology of

corrosion. Corrosion inhibitors remain one of the most practical approaches for controlling this deterioration because they can form an adsorbed or reaction-derived barrier that limits access of aggressive species to electrochemically active sites [1–4]. Recent corrosion-inhibitor research has increasingly emphasized formulations that combine effective surface protection with lower environmental impact. Reviews published during 2022–2025 highlight the growing interest in biodegradable organic compounds, plant-derived inhibitors, polymeric inhibitors and other environmentally preferable alternatives for carbon steel [1,5–8]. In water and cooling-water applications, electrochemical impedance measurements, polarization techniques and surface characterization are frequently used together to distinguish changes in charge-transfer kinetics from actual protective-film formation [2,3,9–12]. Carboxylate-containing compounds are particularly relevant to aqueous corrosion control because oxygen donor atoms can interact with iron-containing surface species. Sodium gluconate is a water-soluble carboxylate with multiple hydroxyl groups and has previously been investigated as a corrosion and scale inhibitor for ordinary steel in simulated cooling water. The reported protection was attributed mainly to adsorption and formation of a surface inhibitive layer [13]. The present study extends this concept to a natural groundwater environment and examines whether Mn^{2+} can act synergistically with sodium gluconate [22,24].

Synergistic inhibitor systems are of great interest because one component can facilitate transport, adsorption or film formation of another component, thereby producing protection greater than that expected from either component alone. Recent work on mixed inhibitor systems and inhibitor combinations has demonstrated that the interaction between components can substantially alter surface-film resistance and corrosion kinetics [9,10,14]. In particular, current research on cooling-water corrosion shows that the effectiveness of an inhibitor depends strongly on water chemistry, pH, film stability and the interaction among treatment chemicals [9,10,15].

The objective of the present study is therefore to evaluate the synergistic effect of sodium gluconate and Mn^{2+} ions on the corrosion of carbon steel in groundwater using gravimetric and electrochemical methods, supported by FTIR and microscopic examination. The concentration dependence, immersion-time effect, pH dependence and synergism parameter are considered, and the results are compared with recent literature on carbon-steel corrosion inhibition. The proposed mechanism involves formation of an Fe^{2+}–gluconate complex at anodic sites and $Mn(OH)_2$ at cathodic sites, producing a composite protective film.

2. Materials and Methods

2.1 Carbon-steel specimens and groundwater

Carbon-steel specimens having the composition 0.15% C, 0.40% Mn, 0.06% P, 0.025% S and balance Fe were used. Rectangular specimens of dimensions 1.0 × 4.0 × 0.2 cm were polished to a mirror finish, degreased with trichloroethylene and used for gravimetric and surface-examination experiments. Groundwater was collected from Tirunelveli, Tamil Nadu, India. The measured groundwater parameters are listed in Table 1.

Table 1. Physicochemical characteristics of the groundwater used in the study.

Parameter	Value
pH	8.0
Total dissolved solids	810 mg L^{-1}
Alkalinity	389 mg L^{-1}
Chloride	15 mg L^{-1}
Sulphate	17 mg L^{-1}
Calcium	82 mg L^{-1}
Magnesium	92 mg L^{-1}
Barium	14 mg L^{-1}

2.2 Weight-loss measurements

Triplicate carbon-steel specimens were

immersed in 100 mL of groundwater containing selected concentrations of sodium gluconate in the absence and presence of Mn^{2+} for three days. Specimens were weighed before and after exposure using a Shimadzu AY62 balance. Corrosion products were removed with Clarke's solution before the final weighing. The inhibition efficiency (IE) was calculated using the expression reported in the original study:

$$IE(\%) = 100\left[1 - \left(\frac{CR_i}{CR_o}\right)\right]$$

where CR_0 is the corrosion rate of the uninhibited specimen and CR_i is the corrosion rate in the presence of inhibitor.

2.3 Potentiodynamic polarization

Polarization measurements were performed using a CHI 66A electrochemical workstation in a conventional three-electrode cell. The carbon-steel specimen was the working electrode, with an exposed area of 1 cm^2; a saturated calomel electrode (SCE) served as the reference electrode and platinum foil as the counter electrode. Corrosion potential (E_corr), corrosion current density (I_corr), anodic and cathodic Tafel slopes and polarization resistance (R_p) were obtained from the polarization curves.

2.4 Electrochemical impedance spectroscopy

AC impedance measurements were conducted using the same three-electrode configuration. The real (Z′) and imaginary (Z″) components of impedance were recorded over the applied frequency range. Charge-transfer resistance (R_ct) and double-layer capacitance (C_dl) were obtained from the impedance response. An increase in R_ct together with a decrease in C_dl was interpreted as evidence of formation of a more resistive interfacial film.

2.5 FTIR and surface morphology

FTIR spectra were recorded using a Perkin–Elmer 1600 spectrophotometer. The surface film was carefully removed from the exposed steel, mixed with KBr and pressed into pellets for spectral analysis. Surface morphology was examined by optical/SEM imaging. The SEM images were obtained using a Hitachi S-450 instrument operated at 15 kV, as described in the original experimental record.

2.6 Effect of immersion time, pH and synergism

The influence of immersion time was examined from 1 to 7 days and the influence of pH was examined between pH 6 and 12. The synergistic interaction between SG and Mn^{2+} was assessed using the synergism parameter S_1 based on the surface-coverage relationship reported in the original study. Values of S_1 greater than unity were taken as evidence of synergism.

3. Results and Discussion

3.1 Groundwater chemistry and corrosion environment

The groundwater used in this work was mildly alkaline (pH 8.0) and contained appreciable dissolved solids. The chloride concentration was relatively low (15 mg L^{-1}), whereas calcium and magnesium were present at 82 and 92 mg L^{-1}, respectively. Under these aerated conditions, oxygen reduction can sustain the cathodic reaction while iron dissolution proceeds anodically. The measured corrosion rate of the uninhibited carbon steel was reported as 13.64 mdd for the three-day reference condition. Recent studies emphasize that inhibitor performance in water systems is highly dependent on water composition, pH, flow, ionic strength and the stability of the interfacial film [9–12,15].

3.2 Weight-loss behaviour and concentration dependence

The gravimetric results demonstrate that sodium gluconate and Mn^{2+} individually provide corrosion protection, while their combination gives substantially higher reported inhibition. At 100 ppm SG alone, the reported inhibition efficiency was 51.21%, whereas 100 ppm Mn^{2+} alone gave 67.53%. With 50 ppm Mn^{2+} present, increasing SG concentration produced a strong improvement in the reported

protection, reaching 97.56% at 200 ppm SG. The optimum composition identified by the original study was therefore 200 ppm SG + 50 ppm Mn^{2+}. The improvement relative to the individual components supports a synergistic interaction rather than simple additive inhibition.

The remaining concentration series in the original dataset are reproduced in Table 4. They show that increasing Mn^{2+} concentration does not produce a monotonic increase in protection at a fixed SG concentration. For example, the highest reported performance occurs at 50 ppm Mn^{2+} with 200 ppm SG, whereas at 100, 150 and 200 ppm Mn^{2+} the reported efficiencies at 200 ppm SG are 70.73, 39.21 and 84.33%, respectively. This non-monotonic behaviour is consistent with the principle that inhibitor combinations have an optimum composition: excess metal ions may change speciation, precipitation, transport or surface competition rather than continuously improving film coverage.

Table 2. Reported corrosion rates and inhibition efficiencies for SG in groundwater in the absence of Mn^{2+} (3 days).

SG (ppm)	Mn^{2+} (ppm)	CR (mdd)	Reported IE (%)
0	0	13.64	–
50	0	12.49	10.36
100	0	6.52	51.21
150	0	4.57	30.48
200	0	5.04	43.29

Table 3. Reported corrosion rates and inhibition efficiencies at 50 ppm Mn^{2+} (3 days).

SG (ppm)	Mn^{2+} (ppm)	CR (mdd)	Reported IE (%)
0	50	9.64	50.60
50	50	8.33	57.31
100	50	0.95	95.12
150	50	4.41	97.43
200	50	0.47	97.56

Table 4. Reported corrosion rates and inhibition efficiencies for SG–Mn^{2+} combinations (3 days).

Mn^{2+} (ppm)	SG (ppm)	CR (mdd)	Reported IE (%)
100	0	6.30	67.53
100	50	7.26	62.80
100	100	3.20	83.53
100	150	2.14	89.02
100	200	5.71	70.73
150	0	15.52	30.48
150	50	19.04	2.43
150	100	9.76	50.00
150	150	2.26	88.41
150	200	11.86	39.21
200	0	12.73	34.75
200	50	10.95	43.90
200	100	13.33	31.70
200	150	5.95	69.51
200	200	3.06	84.33

The high performance of the 200 ppm SG + 50 ppm Mn^{2+} formulation is noteworthy in the context of recent carbon-steel inhibitor research. Zheng et al. reported about 97% inhibition for an ecofriendly dendritic polymer in soft water [2], while De Ketelaere et al. reported up to 98–99% inhibition using sodium silicate under static and flowing saline conditions [12]. By contrast, carboxymethylated dextran reached 82.52% in circulating cooling water [13], and a recent study of HEDP in a power-plant cooling-water system reported a maximum of 58% under long-duration bench conditions [17]. These comparisons should not be interpreted as a direct ranking because the inhibitor chemistry, steel grade, water composition, temperature, hydrodynamics and exposure times differ substantially. Nevertheless, they indicate that the reported 97.56% performance of SG–Mn^{2+} is within the upper range of efficiencies reported for modern aqueous carbon-steel inhibitor systems.

3.3 Potentiodynamic polarization

The polarization response of carbon steel changed markedly after addition of 200 ppm SG and 50 ppm Mn^{2+}. The reported corrosion potential shifted from −0.465 V for the blank groundwater to −0.522 V vs SCE in

the inhibited solution, while I_corr decreased from 4.98 × 10^{-3} to 0.88 × 10^{-3} A cm^{-2}. The cathodic and anodic Tafel slopes also changed, indicating modification of the interfacial kinetics. Because the shift in E_corr is moderate and both branches are affected, the formulation is more appropriately described as having mixed inhibition with a pronounced cathodic influence, rather than as a purely cathodic inhibitor. This interpretation is consistent with recent studies in which mixed inhibitor systems reduce both anodic dissolution and cathodic reduction through formation of a blocking surface film [2,16,18,27].

Table 5. Polarization parameters reported for carbon steel in groundwater.

System	E_corr (V vs SCE)	I_corr (A cm^{-2})	b_c	b_a	R_p (Ω cm^2)
Blank	−0.465	4.98 × 10^{-3}	186.85	153.55	9
SG 200 ppm + Mn^{2+} 50 ppm	−0.522	0.88 × 10^{-3}	158.32	106.33	314

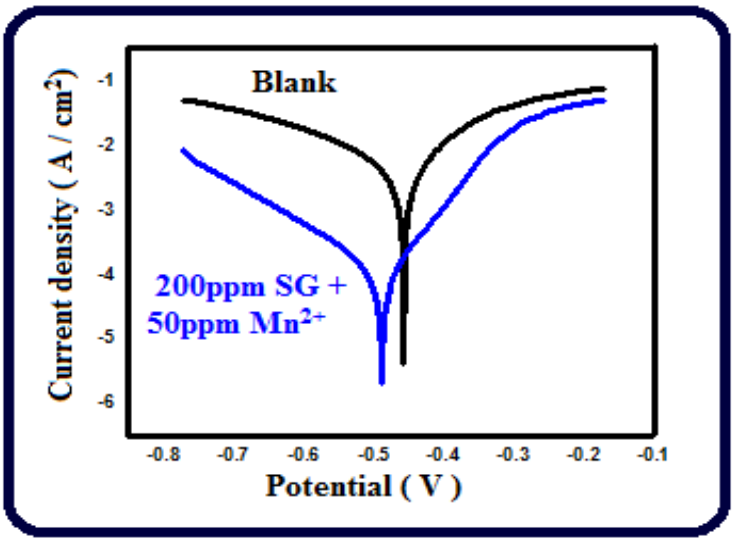


Figure 1. Potentiodynamic polarization curves of carbon steel in groundwater in the absence and presence of 200 ppm SG + 50 ppm Mn^{2+}.

An important editorial point is that the original table lists 97.56% as the polarization inhibition efficiency. However, the I_corr values themselves correspond to a lower percentage reduction when calculated directly from the displayed current densities. Accordingly, the present manuscript treats 97.56% as the reported gravimetric optimum and avoids assigning that same value to the polarization-derived current-density reduction. The raw electrochemical data should be checked against the original laboratory records before final journal submission.

3.4 Electrochemical impedance spectroscopy

The impedance results provide strong evidence for formation of a protective interfacial layer. For the blank groundwater, R_ct was 5.12 Ω cm^2 and C_dl was 1.7 × 10^{-2} F cm^{-2}. After addition of 200 ppm SG and 50 ppm Mn^{2+}, R_ct increased to 298.345 Ω cm^2, whereas C_dl decreased to 1.3 × 10^{-5} F cm^{-2}.

Such a large increase in charge-transfer resistance indicates that electron transfer associated with corrosion was strongly hindered. The reduction in C_dl is also consistent with replacement of interfacial water and/or formation of a thicker, less permeable surface film. Comparable interpretations are widely used in recent inhibitor studies, where increased R_ct and reduced C_dl accompany adsorption or reaction-derived protective layers [2,17,18,20].

3.5 FTIR evidence for the protective film

The FTIR spectrum of sodium gluconate showed a carbonyl-related band at approximately 1548 cm^{-1}, while the film collected from carbon steel exposed to 200 ppm SG + 50 ppm Mn^{2+} exhibited a shift to approximately 1536 cm^{-1}. The shift was interpreted in the original study as evidence for coordination of the carboxylate oxygen with iron to form an Fe^{2+}–gluconate surface complex. A further band near 1411 cm^{-1} was assigned to $Mn(OH)_2$. Together with the impedance results,
these observations support a composite-film model involving an iron–gluconate species on anodic regions and manganese hydroxide on cathodic regions. Recent work on carbon-steel inhibitors similarly demonstrates that oxygen-

Table 6. AC impedance parameters reported for carbon steel in groundwater.

System	R_s (Ω cm^2)	R_ct (Ω cm^2)	C_dl (F cm^{-2})	Reported IE (%)
Blank	2.568	5.12	1.7×10^{-2}	–
SG 200 ppm + Mn^{2+} 50 ppm	−12.402	298.345	1.3×10^{-5}	97.56

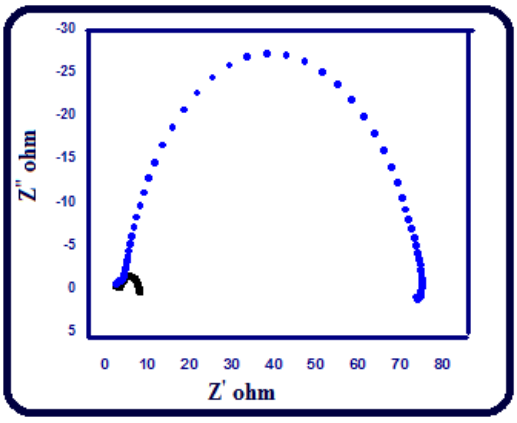


Figure 2. AC impedance response of carbon steel in groundwater in the presence of 200 ppm SG + 50 ppm Mn^{2+}.

containing functional groups can contribute to interfacial film formation, although the exact chemical identity of a film should ideally be confirmed by complementary techniques such as XPS or Raman spectroscopy [17,18,21,25,26].

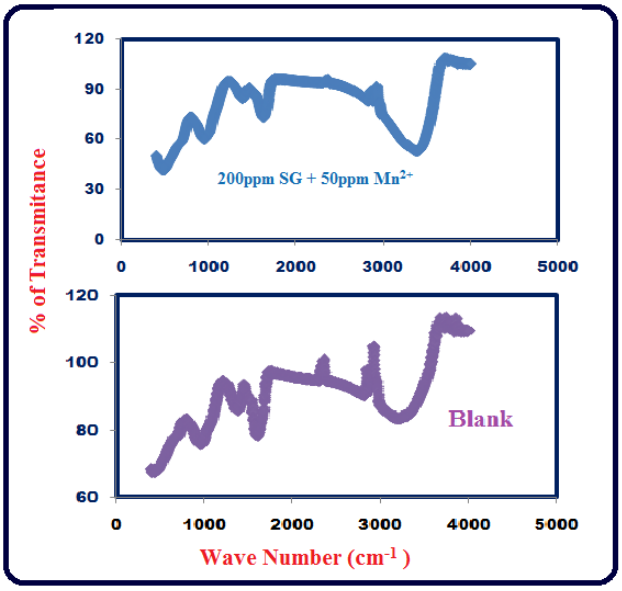


Figure 3. FTIR spectra of the uninhibited and inhibited carbon-steel surface films.

3.6 Surface morphology

The surface images show a marked difference between the uninhibited and inhibited specimens. The carbon steel exposed to groundwater without inhibitor displays a comparatively rough, heterogeneous corrosion-product layer, whereas the specimen exposed to 200 ppm SG + 50 ppm Mn^{2+} shows a more compact and comparatively uniform surface. This morphological difference supports the electrochemical evidence for formation of a protective layer. Comparable correlations between smoother surfaces, higher charge-transfer resistance and lower corrosion rates have been reported for recent green and hybrid inhibitor systems [18,20,22,27].

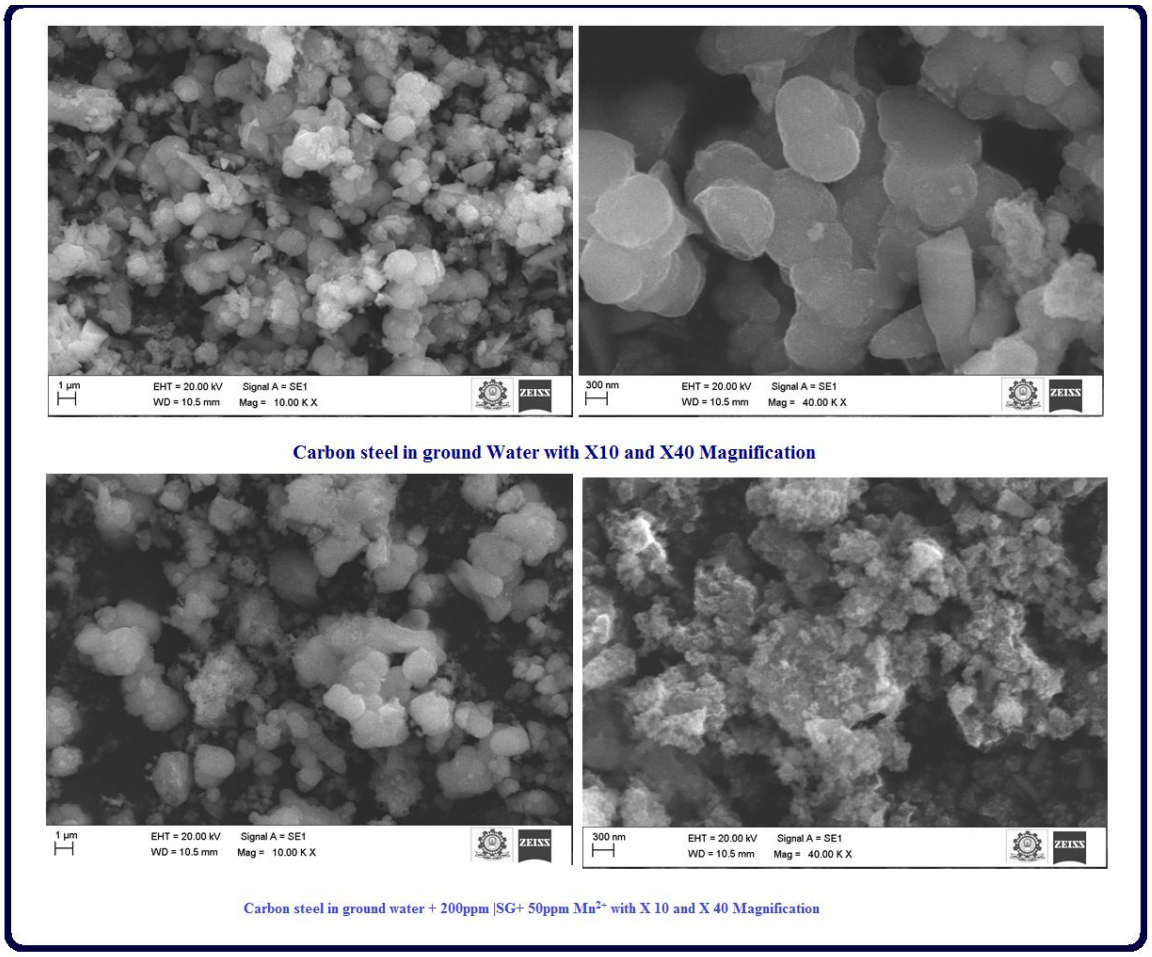


Figure 4. SEM images of carbon steel after three days in groundwater: (top) uninhibited specimen and (bottom) specimen containing 200 ppm SG + 50 ppm Mn^{2+}.

3.7 Effect of immersion time

The reported inhibition efficiency was 48.90% after one day, increased to 97.56% after three days, and then decreased to 87.88% and 90.48% after five and seven days, respectively. The initial increase can be associated with progressive establishment of the protective SG–Mn^{2+} film. The subsequent decrease suggests that the film is not completely invariant during prolonged exposure. Chloride and other dissolved species can compete for surface sites, while local film dissolution, restructuring or corrosion-product accumulation can alter the interfacial composition. Recent long-duration cooling-water studies similarly emphasize that inhibitor performance is not determined solely by the initial efficiency and that film stability under realistic water chemistry is critical [9,10,19]

Table 7. Reported effect of immersion time on the SG–Mn^{2+} system.

Immersion time (day)	Blank CR (mdd)	Inhibited CR (mdd)	Reported IE (%)
1	10.32	10.56	48.90
3	13.64	0.47	97.56
5	15.76	1.25	87.88
7	17.86	1.85	90.48

3.8 Effect of pH

The original dataset reports inhibition efficiencies of 88%, 97%, 90% and 92% at pH

6, 8, 10 and 12, respectively, with the highest protection at the native groundwater pH of 8. The reduction at pH 6 was attributed to increased acidic attack on the steel surface. At higher pH, Mn^{2+} can undergo hydroxide precipitation, potentially reducing its transport to the steel surface; at still higher alkalinity, changes in manganese hydroxo-speciation may alter transport and film formation. Because metal-ion speciation and inhibitor adsorption are strongly pH dependent, the observed maximum at pH 8 is chemically plausible and highlights the importance of optimizing the formulation for the actual water chemistry [3,9,15].

Table 8. Reported effect of pH on the SG–Mn^{2+} system.

pH	Blank CR (mdd)	Inhibited CR (mdd)	Reported IE (%)
6	9.65	1.10	88
8	8.62	0.25	97
10	7.33	1.63	90
12	8.55	1.28	92

Note: the original draft labels the inhibited formulation in this table inconsistently as 'CG150 ppm + Al^{3+} 100 ppm', although the section heading identifies the SG–Mn^{2+} system. For consistency with the study objective and surrounding results, the table above uses the SG–Mn^{2+} designation. This should be verified against the laboratory notebook before submission.

3.9 Synergistic interaction

The calculated synergism parameter S_1 was reported to be greater than unity for the SG–Mn^{2+} combinations, supporting a synergistic rather than merely additive effect. For 200 ppm SG + 50 ppm Mn^{2+}, the reported S_1 value was 6.19. Such strong positive interaction can reasonably be associated with complementary roles of the two components: gluconate can provide oxygen-donor coordination and facilitate interfacial transport of Mn^{2+}, while the released Mn^{2+} can form $Mn(OH)_2$ under cathodic conditions. Mixed-component protection of this type is consistent with the broader literature showing that optimized combinations can produce more coherent or persistent films than single inhibitors [9,10,14,18].

Table 9. Reported synergism parameters for SG–Mn^{2+} combinations.

SG (ppm)	SG IE (%)	Mn^{2+} (ppm)	Mn^{2+} IE (%)	Combined IE (%)	S_1
50	10.36	50	15.2	57.31	2.31
100	51.21	50	15.2	95.15	7.55
150	30.48	50	15.2	77.43	5.45
200	43.29	50	15.2	97.56	6.19

3.10 Proposed inhibition mechanism

The experimental observations support the following mechanistic sequence. First, sodium gluconate and Mn^{2+} interact in the groundwater to form soluble or weakly associated Mn^{2+}–gluconate species. Second, these species are transported from the bulk solution toward the steel surface. Third, at anodic regions, Fe^{2+} generated by iron dissolution can interact with gluconate to produce an Fe^{2+}–gluconate surface complex. The Mn^{2+} released during this exchange can be transported toward cathodic regions where locally generated OH^- promotes formation of $Mn(OH)_2$. The combined Fe^{2+}–gluconate/$Mn(OH)_2$ film reduces access of water and aggressive ions to active sites and increases the interfacial resistance to charge transfer.

$$Mn^{2+}\text{–SG} + Fe^{2+} \rightarrow Fe^{2+}\text{–SG} + Mn^{2+}$$

$$Mn^{2+} + 2OH^- \rightarrow Mn(OH)_2$$

This mechanism should be regarded as a working interpretation rather than a complete molecular description. Direct identification of Fe, Mn and oxygen chemical states by XPS, together with elemental mapping and cross-sectional film analysis, would provide stronger evidence for the proposed film composition.

4. Comparison with Recent Literature

Recent literature confirms that carbon-steel corrosion inhibition in aqueous systems increasingly relies on film-forming organic, inorganic and hybrid inhibitors. The present SG–Mn^{2+} formulation is particularly interesting because its reported optimum efficiency is comparable with some high-performing modern systems while using a relatively simple combination of a water-soluble carboxylate and a divalent metal ion.

The comparison indicates that the reported 97.56% efficiency of the present formulation is competitive with several recent high-efficiency systems. Importantly, the comparison also reveals why inhibition efficiency alone should not be used to rank formulations: a 97% result obtained after three days in groundwater cannot be directly equated with a 58% result obtained after 1000 h in power-plant cooling water. Long-term stability, compatibility with scale control and biocides, toxicity, biodegradability, cost, water chemistry and field hydrodynamics must all be considered before industrial implementation [9,19]. Recent reviews further emphasize that the next generation of inhibitors should combine effective barrier formation with reduced environmental impact [1,5,7,8].

Table 10. Comparison of the present SG–Mn^{2+} system with selected recent carbon-steel inhibitor studies.

Study	Environment / material	Inhibitor system	Maximum reported IE	Main evidence
Present work	Groundwater; carbon steel	SG 200 ppm + Mn^{2+} 50 ppm	97.56%	Weight loss, polarization, EIS, FTIR, SEM
Zheng et al. (2023) [2]	Soft water; carbon steel	ITCP dendritic polymer	~97%	Weight loss, Tafel, EIS
De Ketelaere et al. (2024) [12]	Saline water; carbon steel	Sodium silicate	98–99%	Polarization, EIS, Mott–Schottky
Xu & Chen (2024) [13]	Circulating cooling water; carbon steel	Carboxymethylated dextran	82.52%	Weight loss, electrochemistry, surface analysis
K. Vignesh et al. (2024) [23]	Cooling-tower water; API 5LX	N-substituted tetrabromophthalic inhibitors	~79% (WL)	Weight loss, electrochemistry, biofilm assay
Biedunkova et al. (2025) [16]	Power-plant cooling water; St-20	HEDP	58%	1000 h weight-loss bench test
Fouda et al. (2025) [17]	0.5 M H_2SO_4; API 5L X70	Cuminum cyminum extract	91.83%	WL, PDP, EIS, SEM/AFM

5. Conclusions

1. The sodium gluconate–Mn^{2+} combination exhibits a strong synergistic corrosion-inhibition effect for carbon steel exposed to the investigated groundwater.
2. The optimum formulation identified in the original experimental dataset is 200 ppm sodium gluconate + 50 ppm Mn^{2+}, for which a maximum reported inhibition efficiency of 97.56% was obtained after three days.
3. Polarization and impedance measurements indicate substantial suppression of corrosion kinetics and formation of a protective interfacial film. The electrochemical response is best described as mixed inhibition with a pronounced cathodic influence.

4. The large increase in R_ct from 5.12 to 298.345 Ω cm² and the decrease in C_dl from 1.7 × 10^{-2} to 1.3 × 10^{-5} F cm^{-2} are consistent with formation of a compact, resistive surface layer.
5. FTIR and microscopy support a film-forming mechanism involving an Fe^{2+}–gluconate complex and $Mn(OH)_2$, although complementary surface-chemical measurements are required for definitive identification.
6. The inhibition efficiency depends on inhibitor composition, immersion time and pH, demonstrating the importance of optimizing the formulation for the actual water chemistry.
7. The reported performance is competitive with several recent carbon-steel inhibitor systems, but longer-term field-relevant testing is necessary before industrial deployment.

References

[1] Desai P.D., Pawar C.B., Avhad M.S., More A.P., Corrosion inhibitors for carbon steel: A review, Vietnam Journal of Chemistry 61 (2023) 15–42. https://doi.org/10.1002/vjch.202200111.

[2] Zheng H., Zhang B., Wang X., Lu Y., Li F., Li C., Improved corrosion resistance of carbon steel in soft water with dendritic-polymer corrosion inhibitors, Chemical Engineering Journal 452 (2023) 139043. https://doi.org/10.1016/j.cej.2022.139043.

[3] Alao A.O., Popoola A.P., Dada M.O., Sanni O., Utilization of green inhibitors as a sustainable corrosion control method for steel in petrochemical industries: A review, Frontiers in Energy Research 10 (2023) 1063315. https://doi.org/10.3389/fenrg.2022.1063315.

[4] Yu H., Ge H., Zhang J., Li J., Liu J., Zhao Y., Corrosion inhibition of hydrazine on carbon steel in water solutions with different pH adjusted by ammonia, Corrosion Reviews 40 (2022) 587–596. https://doi.org/10.1515/corrrev-2022-0029.

[5] Fazal B.R., Becker T., Kinsella B., Lepkova K., A review of plant extracts as green corrosion inhibitors for CO_2 corrosion of carbon steel, npj Materials Degradation 6 (2022) 5. https://doi.org/10.1038/s41529-021-00201-5.

[6] Jero D., Caussé N., Pébère N., Film-forming amines as corrosion inhibitors: a state-of-the-art review, npj Materials Degradation 8 (2024) 111. https://doi.org/10.1038/s41529-024-00523-0.

[7] Galleguillos Madrid F.M., Soliz A., Cáceres L., Bergendahl M., Leiva-Guajardo S., Portillo C., Olivares D., Toro N., Jimenez-Arevalo V., Páez M., Green Corrosion Inhibitors for Metal and Alloys Protection in Contact with Aqueous Saline, Materials 17 (2024) 3996. https://doi.org/10.3390/ma17163996.

[8] Holla B.R., Mahesh R., Manjunath H.R., Anjanapura V.R., Plant extracts as green corrosion inhibitors for different kinds of steel: A review, Heliyon 10 (2024) e33748. https://doi.org/10.1016/j.heliyon.2024.e33748.

[9] Lu S., Li X., Zheng X., Zhao H., Tian Z., Tang G., Lei R., Zhuang P., Wei T., Wu S., Electrochemical effects on carbon steel in circulating cooling water systems: Scaling, corrosion and chemicals synergies, Journal of Water Process Engineering 63 (2024) 105337. https://doi.org/10.1016/j.jwpe.2024.105337.

[10] Optimization and understanding of corrosion inhibitors for cooling water system, Anti-Corrosion Methods and Materials 70 (2023) 259–267. https://doi.org/10.1108/ACMM-02-2023-2754.

[11] Liu S., Zhou J., Liang G., Lyu X., Li Z., Evaluation of green corrosion inhibitors of chitosan oligosaccharide derivatives for CO_2 corrosion inhibition on 20# carbon steel, Process Safety and Environmental Protection 190 (2024) 1520–1535. https://doi.org/10.1016/j.psep.2024.07.052.

[12] De Ketelaere E., Moed D., Verbeken K., Depover T., A comprehensive electrochemical evaluation of the corrosion

inhibition by sodium silicate on carbon steel, Electrochimica Acta 507 (2024) 145053. https://doi.org/10.1016/j.electacta.2024.145053.

[13] Xu P., Chen X., Inhibition of Carbon Steel Corrosion Using Dextran Derivatives in Circulating Cooling Water, Water 16 (2024) 1182. https://doi.org/10.3390/w16081182.

[14] Banumathi R., Abuthahir S.S.S., Sheit H.M.K., Mohan K.S., Mohandas T., Vijaya K., Corrosion inhibition potential of aqueous extract of Trifolium repens plant leaves on carbon steel in hydrochloric acid medium (TRPL), Discover Electrochemistry 1 (2024) 13. https://doi.org/10.1007/s44373-024-00014-6.

[15] Parangusan H., Sliem M.H., Abdullah A.M., Elhaddad M., Al-Thani N., Bhadra J., Plant extract as green corrosion inhibitors for carbon steel substrate in different environments: A systematic review, International Journal of Electrochemical Science 20 (2025) 100919. https://doi.org/10.1016/j.ijoes.2024.100919.

[16] Biedunkova O., Kuznietsov P., Martynov S., Kucherova A., Hrytsyna O., Bench-scale performance evaluation of phosphonate (HEDP) for corrosion inhibition of carbon steel in a power plant cooling water system, Engineering Reports 7 (2025) e70473. https://doi.org/10.1002/eng2.70473.

[17] Fouda A.S., Rashwan S., Ibrahim H., Reda M., Eissa M.E., El-Hossiany A., Cuminum cyminum as green corrosion inhibitor for API 5L X70 carbon steel in 0.5 M H_2SO_4 solution, Scientific Reports 15 (2025) 17120. https://doi.org/10.1038/s41598-025-

[18] Suliman A.E., Mangood A.H., Yehia N.S., Abdelraouf M., Batakoushy H.A., Abdou .M., Zaki E.G., Gallic acid based green 98407-z.

corrosion inhibitor for mild steel in 1 M HCl: electrochemical and microbial assessment with theoretical validation, Scientific Reports 15 (2025) 15156. https://doi.org/10.1038/s41598-025-97647-3.

[19] Rajendran S., Apparao B.V., Palaniswamy N., Anticorrosion methods and materials 49 (2002) 205. DOI: https://doi.org/10.1108/00035590210426472

[20] Rajendran S., Shanmugapriya S., Rajalakshmi T., John Amalraj A., Corrosion 61 (2005) 685.

[21] Holness R.J., Williams G., Worsley D.A., McMurray H.N., Journal of The Electrochemical Society 152 (2005) B73. DOI: https://doi.org/10.1149/1.1850857 cronfa.swan.ac.uk

[22] Foley R.T., Corrosion 26 (1970) 58. https://doi.org/10.5006/0010-9312-26.2.58

[23] Vignesh, K., Sujithra, S., Vajjiravel, M., Narenkumar, J., Das, B., AlSalhi, M. S., Devanesan, S., Rajasekar, A., & Malik, T., Scientific Reports, 14, Article 25408 (2024). DOI: https:// doi.org/10.1038/s41598-024-76254-8

[24] Wranglen G., Introduction to Corrosion and Protection of Metals, Chapman & Hall, London, 1985. https://doi.org/10.1007/978-94-009-4850-1

[25] Silverstein R.M., Bassler G.C., Morrill T.C., Spectrometric Identification of Organic Compounds, John Wiley & Sons, New York, 1981. ISBN: 978-0471029908

[26] Nakamoto K., Infrared and Raman Spectra of Inorganic and Coordination Compounds, Wiley-Interscience, New York, 1986. https://doi.org/10.1002/9780470405840

[27] Giacomelli F.C., Giacomelli C., Amadori M.F., Schmidt V., Spinelli A., Materials Chemistry and Physics 83 (2004) 124. DOI: https://doi.org/10.1016/j.matchemphys.2003.09.013